

Prepreg forming, curing and structural analysis for an aero engine component

Dennis Wilhelmsson¹, Jesper Eman², Vivekendra Singh², Anders Bernhardsson³, Mats Landervik³

¹GKN Aerospace Sweden AB
²RISE Research Institutes of Sweden
³DYNAmore Nordic

1 Introduction

Carbon fibre composites have the potential of reducing weight and thereby the carbon footprint of an aero engine component due to the high strength and stiffness of the material relative to its weight. In this paper, a process simulation chain, consisting of forming, curing and structural simulations, is proposed. The demonstrator here is an outlet guide vane (OGV) which is part of an electric fan aero engine demonstrator, See Fig.1 below. This electric ducted fan (EDF) has been developed by GKN Aerospace Sweden in collaboration with the Royal institute of technology (KTH).

The objective of the simulations is to facilitate the optimization of the guide vane design and production process, by reducing the number physical iterations. It is done early in the design phase by considering the properties resulting from the process in the predictions of the part performance in the use phase. Concretely, forming and curing simulations are used to get a better understanding of the process and predict fibre angles and shape distortions to provide improved accuracy in the subsequent structural simulations.

The OGV is produced by a novel double vacuum forming (DVF) process. In the process, a full stack of prepreg plies is placed on a rubber membrane. The stack is then formed, debulked and consolidated in vacuum at a material specific temperature after which it can be demoulded and moved to the curing tool.



Fig.1: Rendering of the electric ducted fan thruster developed by GKN and KTH.

An illustration of the simulation chain presented in this paper is shown in Fig.2. The forming simulation is the first of three simulation steps from which the resulting mesh and fiber orientations are exported. To have a 3D representation of the plies in the subsequent curing and structural simulations, the shell mesh resulting from forming is inflated in the thickness direction. Second is the curing analysis. Resulting nodal coordinates and residual stresses are subsequently transferred to the third step, the structural simulations.

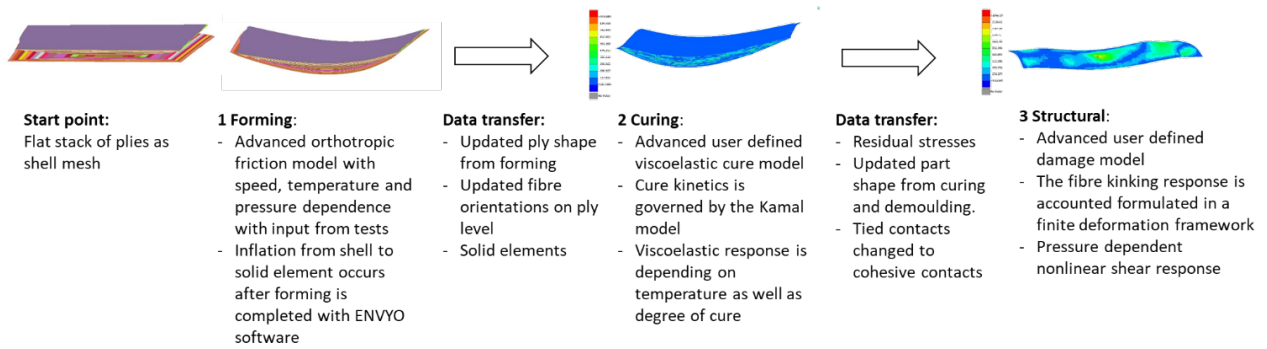


Fig.2: Sequential simulations of a composite vane in LS-Dyna.

2 Forming simulation

2.1 Finite element model

Each of the 42 plies in the stack are modelled as individual parts in the simulation model. The plies are initially flat and the outer shape for each ply has been defined by an inverse modelling method based on the thickness variation of the component. All the plies have the same thickness but with different fiber orientations. The complete forming setup consists of the actual forming tool, frame and rubber membrane, see Fig.3. There is also filler geometry placed between the frame and the tool. The rubber membrane is modelled using *MAT_MOONEY-RIVLIN_RUBBER.

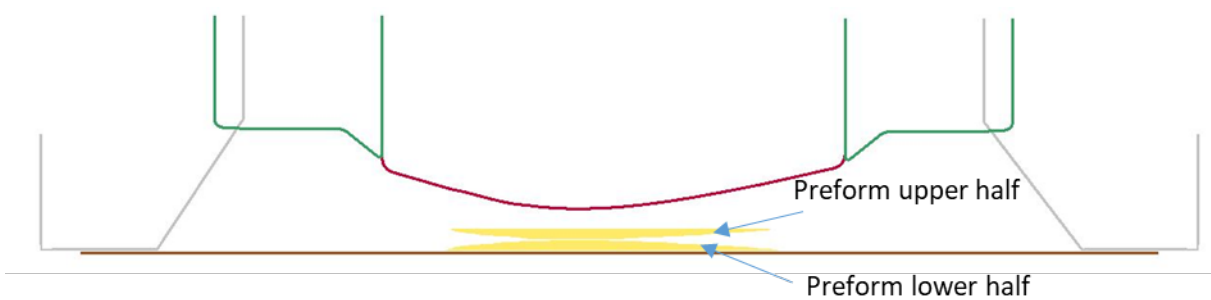


Fig.3: Section cut of the initial setup for the forming simulation.

2.2 Characterization of prepreg material and interply friction

The prepreg plies are modelled with shell elements using their material model *MAT_REINFORCED_THERMOPLASTIC (MAT_249). Physical tests have been performed on the material. Three major deformation mechanisms have been shown to govern the forming of UD Prepreg [1]. They are intra-ply shear, out of plane bending and interply friction. Intra-ply shear, that is shear in the plane of the prepreg was characterized with Bias-Extension test with two cross-plyed laminates to get a force-displacement curve. The test setup is similar to that of [2]. This curve is then used to calibrate the shearing behavior of the plies. The out of plane bending behavior was measured by the cantilever bending test as described by ASTM standard D1388 [3]. Numerically an integration rule for the shell elements (*INTEGRATION_SHELL) is used to calibrate against the physical test.

Interply friction, that is the shear between the layers of the individual prepreps was characterized with the test setup as described in [4]. This characterization was done at different pressures, sliding velocities and sliding directions relative to the fiber directions in the neighboring ply. The contact *CONTACT_AUTOMATIC_SINGLE_SURFACE_MORTAR_ORTHO_FRICTION is used to describe this interaction between the plies. This contact can handle how the friction between the plies varies depending on the fiber orientation and sliding direction. It can also handle dependencies of pressure and sliding velocities [5].

A pressure is applied on the rubber membrane to simulate the vacuum. The membrane deforms and the stack of plies is formed against the forming tool (Fig.4 (a)). The deformed mesh (Fig.4 (b)) is then exported together when the fiber orientation in each ply.

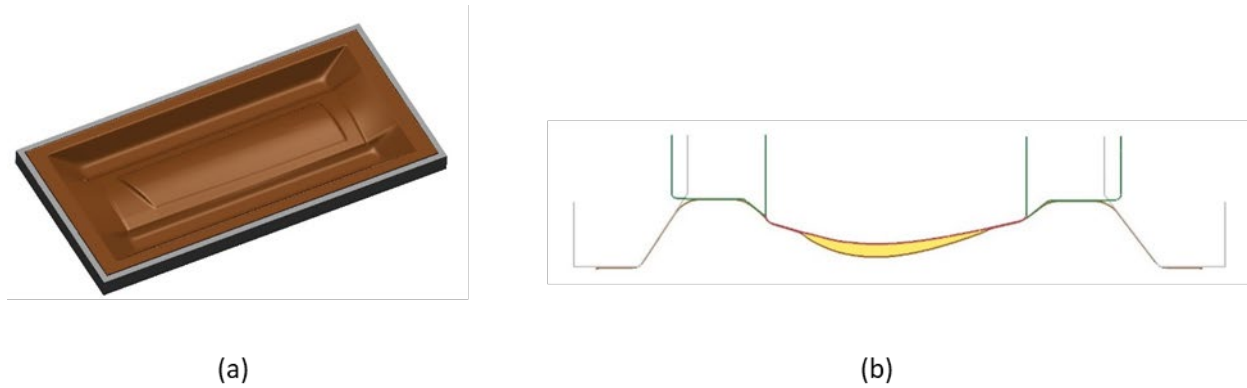


Fig.4: a) CAD model of the forming tool, b) Cross section of the simulation model at the end of forming process.

3 Curing simulation

3.1 Cure simulation model

The cure simulations in the present work employ a user defined subroutine implementing a viscoelastic material model where stress relaxation depends on both temperature and degree of cure [6]. The stress-strain relationship for the material can be described in one dimension as

$$\sigma(t) = \int_{-\infty}^{\psi} E_{rel}(\psi - \psi') \frac{d\varepsilon}{d\psi'} d\psi', \quad (1)$$

where the relaxation modulus is described using a Prony series.

$$E_{rel} = E_{\infty} + \sum_{m=2}^M E_m \exp\left(-\frac{t}{\tau_m}\right) \quad (2)$$

In this equation, the infinite module E_{∞} , the constants E_m and relaxation times τ_m are determined experimentally. ψ is reduced time and is expressed as

$$\psi = \int_{-\infty}^t \frac{dt'}{a(T_c, t_c, T)}, \quad (3)$$

where $a(T_c, t_c, T)$ is the product of the cure shift factor $a_c(T_c, t_c)$ and the temperature shift factor $a_T(T)$. These two shift factors are determined experimentally. The model further incorporates chemical shrinkage, orthotropic thermal and mechanical material properties and uses the Kamal model [8] to determine degree of cure.

3.2 Finite element model

Each ply of the component is modelled as an individual part which results in 42 different parts with tied contacts between them, see Fig.4. The cure simulation would have benefitted from a more homogenous finite element model but since the mesh emerged from the forming simulation, this choice was made. The elements are fully integrated solids, and the entire model consists of roughly 400 000 elements. For each element, the forming analysis has specified an A- and D-vector, defining the local material direction of the ply. This definition for material directions is only working for structural problems which is why a material direction has been defined in the thermal material cards. Further, an individual thermal material

card has been defined for each part which implies that from a thermal point of view, the material directions are the same all over the part but vary between parts.

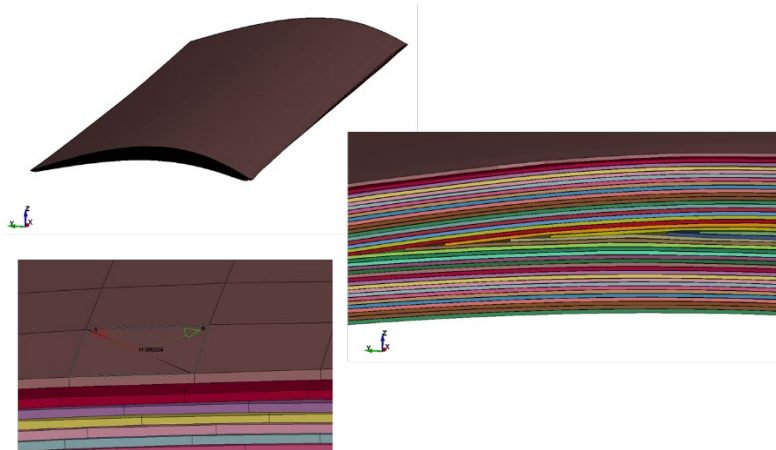


Fig.5: Illustration of the component, the part split and the material directions of a selected element.

To ensure tied, thermal contacts between the plies, *CONTACT_AUTOMATIC_SURFACE_TO_SURFACE_MORTAR_TIED_THERMAL is used between each neighboring layer as well as between selected part interfaces between the upper and lower halves of the stack. Regarding the contact formulations, we see a large potential to improve the accuracy of the results of the model. Especially the contact between the upper and lower preform halves required significant simplifications due to initial convergence problems. The moulding tool is not modelled explicitly, the exterior nodes are instead locked in place during the in-mould cure. These are then released to allow for springback of the component. The thermal boundary conditions are also applied by controlling the temperature of the exterior nodes according to the manufacturers recommended cure cycle.

3.3 Results

The most interesting results from the cure simulation are internal temperatures caused by the exothermal reaction as well as the shape distortions emerging from the cure induced chemical shrinkage and the thermal shrinkage during cool down. Also, the residual stresses are of interest and in this case they are exported as input to the subsequent structural simulation. Fig.6 illustrates the temperatures at the moment when the peak temperature is reached. The exothermal reaction causes the maximum temperature to reach 455.2 K while the tooling temperature is 453.0 K, hence a very small overshoot which should not cause any issues with the quality of the component.

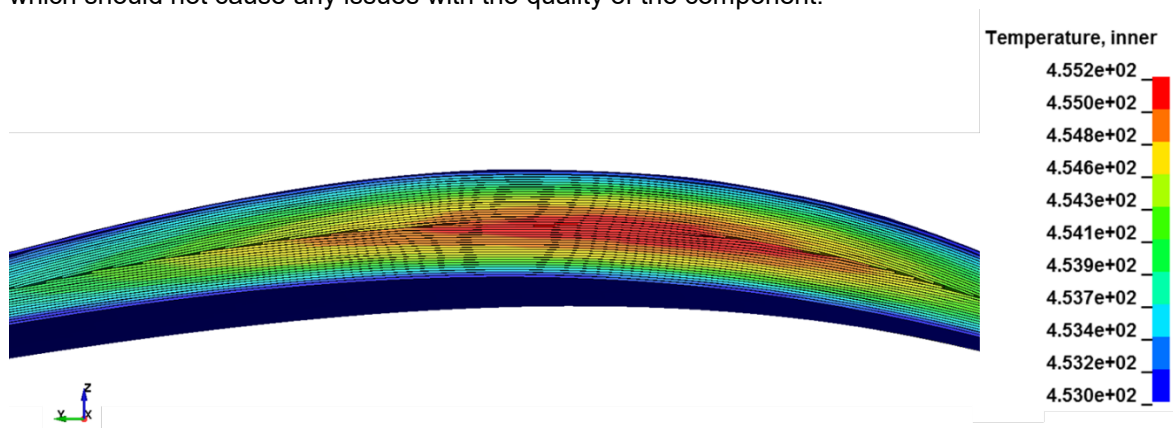


Fig.6: Illustration showing the effects of the exothermal reaction on the spatial temperature distribution for a cross section of the vane.

Fig.7 illustrates the resulting displacements after cure where the maximum displacement is found to be 0.3 mm along one edge of the component. Such a shape distortion should preferably be compensated in the design process before curing tools are manufactured.

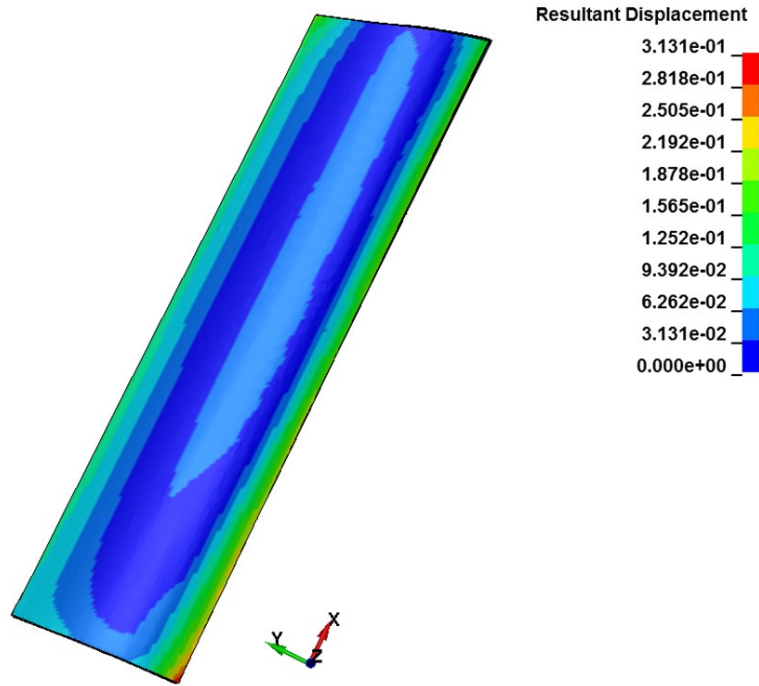


Fig.7: Cure induced shape distortions. Displacements are presented in the unit mm.

4 Structural simulation

4.1 Constitutive model with damage

This section presents briefly the constitutive model for damage growth of the composite. Details of the constitutive models can be found in [7]. A general large strain formulation is applied with a view towards general three-dimensional simulations. The constitutive response in the material coordinate system is then given by:

$$\mathbf{S}^i = \mathbf{C}\mathbf{E}^i \quad (4)$$

where \mathbf{S}^i is the local stress tensor and \mathbf{C} is the stiffness tensor in the material coordinates. \mathbf{E}^i is the local Green–Lagrange (G–L) strain tensor transformed from the global coordinate system to the ‘misalignment’ frame using transformation matrix. The global G–L strain tensor is defined as:

$$\mathbf{E} = \frac{1}{2}(\mathbf{F}^T\mathbf{F} - \mathbf{I}), \quad (5)$$

where \mathbf{F} is the deformation gradient and \mathbf{I} is the second order identity tensor. The nonlinear shear behavior drives both the response in transverse compression and fibre kinking, therefore its accurate characterization and modelling are fundamental for the constitutive modelling of damage growth. To do that, the second Piola–Kirchhoff local stress tensor \mathbf{S}^i expressed in a coordinate system aligned with the ψ -plane, \mathbf{S}^ψ are transformed as:

$$\mathbf{S}^\psi = \mathbf{T}_i^T \mathbf{S}^i \mathbf{T}_i \quad (6)$$

The nonlinear shear response of the material model is obtained by combining damage and friction that occurs at the contact between surfaces of microcracks. The traction vectors in the normal, longitudinal and transverse direction are computed as:

$$\mathbf{S}^\psi = (1 - d)\tilde{\mathbf{S}}^\psi + d\mathbf{S}^{i,\text{fric}} \quad (7)$$

where d is the damage variable, $\tilde{\mathbf{S}}^\psi$ are the components of the stress tensor in the fracture plane, $\mathbf{S}^{i,\text{fric}}$ is the shear stresses associated with friction. The damage, driven by the effective strain E in the critical fracture plane, is given as:

$$d = \frac{(2E)^p - (\gamma_0)^p}{(\gamma_f)^p - (\gamma_0)^p} \quad (8)$$

where γ_0 and γ_f are the strains at damage initiation and at full decohesion, respectively. The exponent p is used to obtain a closer agreement with the experimental shear stress–strain curve. Finally, in order to obtain the global response, the stress tensor in the critical fracture plane needs to be expressed in the global frame according to:

$$\mathbf{S} = \mathbf{T}_\psi^T \mathbf{S}^\psi \mathbf{T}_\psi \quad (9)$$

4.2 Finite element simulation

The test specimen, subjected to different loading conditions is shown in Fig.8². Resulting nodal coordinates and residual stresses from cure simulation are used as an input to perform structural simulations. . Resulting nodal coordinates and residual stresses from cure simulation are used as an input to perform structural simulations.

To capture the interlaminar failure pattern, tied contacts between all adjacent parts *CONTACT_AUTOMATIC_SINGLE_SURFACE_TIED is used. The result of this numerical example is provided in subsection 4.3 (Fig.8). In this project, the material considered will be a linear elastic up to failure initiation and transversely isotropic solid with continuum damage based on the constitutive model explained in section 4.1. However, in this paper, a preliminary model is used for structural simulations with a fully linear elastic material model without the damage constitutive model.

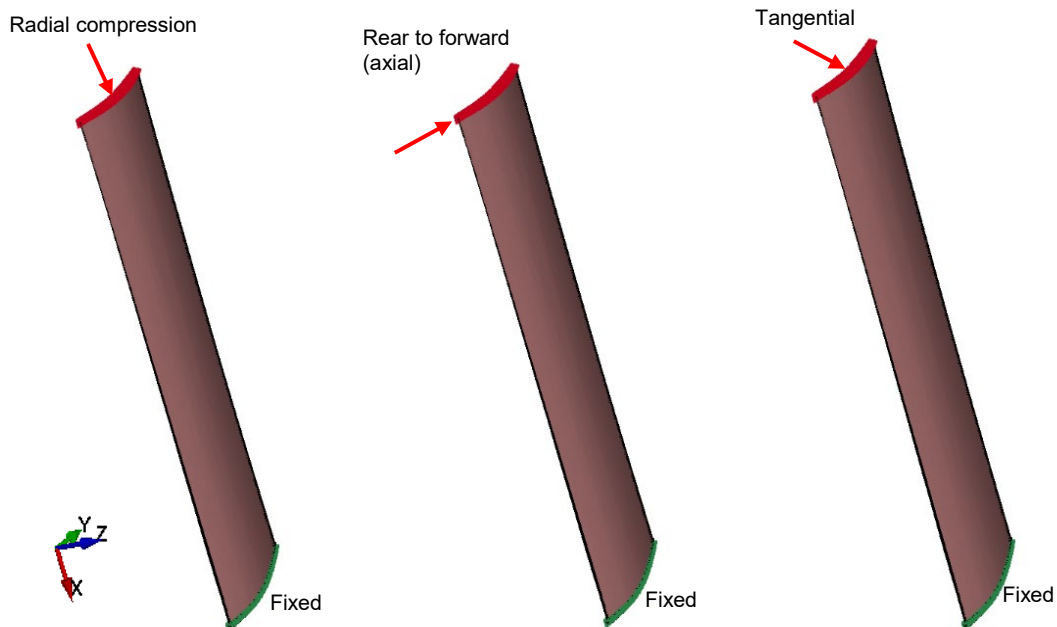


Fig.8: Specimen geometry and boundary conditions of a composite vane (3D FE-model with contacts between each ply) subjected to different displacement loading conditions.

4.3 Results and discussion

The linear elastic material model is used in LS-DYNA for 3D FE-analysis of the OGV. The FE-model is discretized with 8-point hexahedron solid elements. The default element formulation of constant stress solid element was used first, but better results were obtained when using, instead, a fully integrated solid intended for elements with poor aspect ratio with efficient formulation. Fig.8 shows the numerical predictions of effective von Mises stress obtained under different boundary conditions. In radial compression, a localized stress concentration is observed in lower plies of top boundary (Fig.8(a)). A visible stress concentration is observed in upper plies of top boundary under rear-to-forward (axial) loading condition (Fig.8(b)). However, for tangential loading, a stress localization is observed on both edges of lower plies close to the upper boundary (Fig.8(c)). In the future, the proposed constitutive model (section 4.1) will be used for structural analysis to simulate Intra- and Interlaminar failure patterns and validate with experimental results.

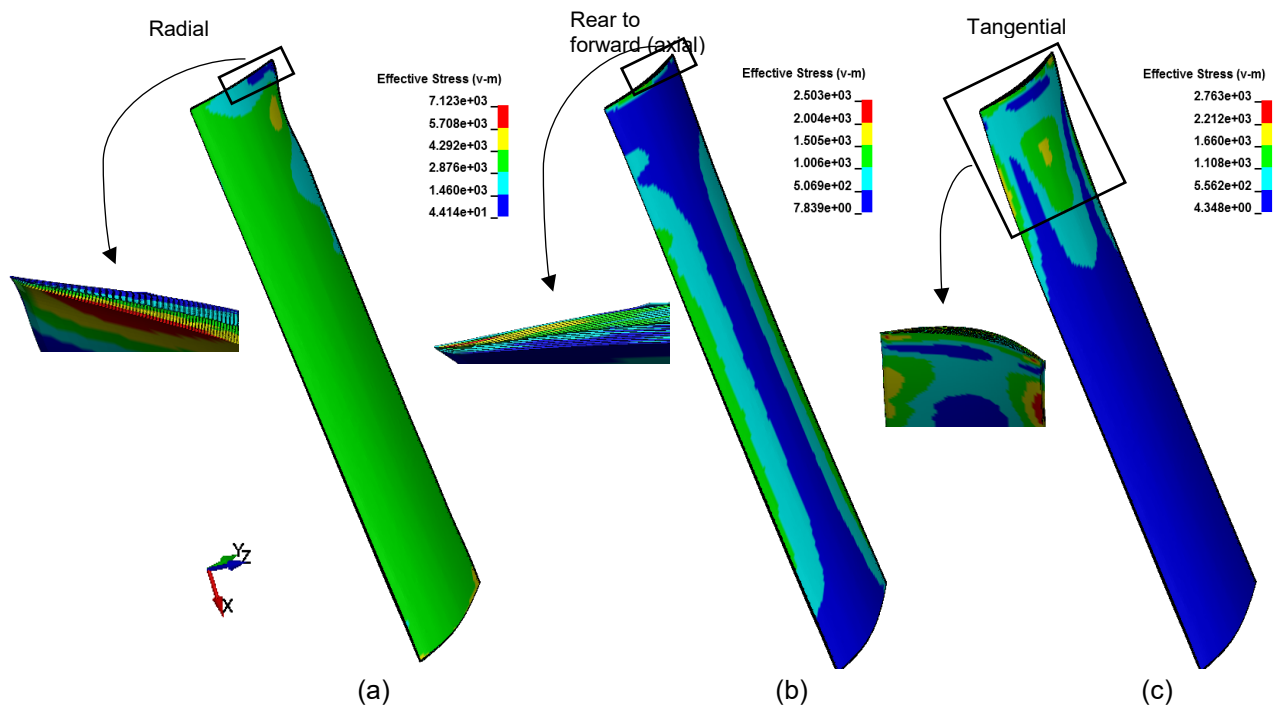


Fig.9: FE predictions of a composite vane subjected to different loading conditions. The stress distribution refer to the maximum from all plies.

5 Data transfer, mapping and meshing

In the current study, the part geometry and properties throughout the process cycle all stem from the input to the forming simulation being the first in the chain, see Fig.1. The input is the geometry of the tool and the original flat shape of the prepreg plies along with material and friction properties. The plies are represented by shell elements in the applied forming simulation methodology while the following curing analysis involves a volume change as the resin changes phase from liquid to rigid. To put less restriction on volume change and deformation, the shell elements are inflated in the thickness direction into solid elements. The ENVYO software [9] is used to transfer the material history variables containing the fiber orientation from the shell forming mesh to material directions in *ELEMENT_SOLID_ORTHO in the solid mesh for curing analysis. The next mesh and data transfer is between curing and structural analyses. In this, nodal coordinates as well as element stresses are output at the last step of the curing analysis and the resulting *NODES and *INITIAL_STRESS_SOLID keywords are included in the structural analysis.

6 Summary

In this paper, a simulation chain methodology, consisting of forming, curing and structural analysis, has been presented. The methodology includes simulations in three steps and the transfer of data, including formed geometry, resulting fiber orientations and residual stresses, between each step. The goal has been to develop this methodology to facilitate the development and reduce the need for physical process iterations of CFRP parts considering all relevant manufacturing steps in the assessment of the product performance in the final use phase. To summarize, advanced material and friction models within three different disciplines has in this project been joined together to create a new method for manufacturing simulations of composites and the subsequent consideration of these in structural assessment.

7 Literature

- [1] Sjölander, J. (2018). Improving Forming of Aerospace Composite Components through Process Modelling (PhD dissertation, KTH Royal Institute of Technology). Retrieved from <https://urn.kb.se/resolve?urn=urn:nbn:se:kth:diva-232841>
- [2] Larberg YR, Åkermo M, Norrby M. On the in-plane deformability of cross-plyed unidirectional prepreg. *Journal of Composite Materials*. 2012;46(8):929-939. doi:10.1177/0021998311412988
- [3] ASTM. Standard test method for stiffness of fabrics; 2008. DOI: 10.1520/D1388-18
- [4] A. Dutta, M.K. Hagnell, M. Åkermo, Interply friction between unidirectional carbon/epoxy prepreg plies: Influence of fibre orientation, *Composites Part A: Applied Science and Manufacturing*, ISSN 1359-835X, <https://doi.org/10.1016/j.compositesa.2022.107375>
- [5] Kumaraswamy, S., Dutta, A., Bernhardsson, A., Landervik, M., Åkermo, M.: "On Interply Friction in Prepreg Forming Simulations." 13th European LS-DYNA Conference, 2021.
- [6] Saseendran, S.: "Effect of Degree of Cure on Viscoelastic Behavior of Polymers and their Composites", PhD dissertation, 2017.
- [7] Costa, S., Zrida, H., Olsson, R., Herráez, M., Östlund, R.: "A unified physically-based finite deformation model for damage growth in composites", 161, 107103, *Composite: Part A*, 2022.
- [8] Kamal M.R., Sourour S.: "Kinetics and thermal characterization of thermoset cure", *Polymer Engineering & Science*. 1973 Jan 1;13(1):59-64.
- [9] Liebold, C., Haufe, A.: "Process2product Simulation: Closing Incompatibilities in Constitutive Modeling and Spatial Discretization with envyo®", 15th International LS-DYNA Conference, 2018.